Rare copy number variations in congenital heart disease patients identify unique genes in left-right patterning

Khalid A. Fakhro[a,b], Murim Choi[a,b], Stephanie M. Ware[c], John W. Belmont[d], Jeffrey A. Towbin[c], Richard P. Lifton[a,b,1], Mustafa K. Khokha[a,e,1], and Martina Brueckner[a,e,1]

[a]Department of Genetics, [b]The Howard Hughes Medical Institute, and [e]Department of Pediatrics, Yale University School of Medicine, New Haven, CT 06520; [c]Department of Pediatrics, Cincinnati Children's Hospital Medical Center, University of Cincinnati College of Medicine, Cincinnati, OH 45229; and [d]Department of Molecular and Human Genetics, Baylor College of Medicine, Houston, TX 77030

Contributed by Richard P. Lifton, January 3, 2011 (sent for review September 21, 2010)

Dominant human genetic diseases that impair reproductive fitness and have high locus heterogeneity constitute a problem for gene discovery because the usual criterion of finding more mutations in specific genes than expected by chance may require extremely large populations. Heterotaxy (Htx), a congenital heart disease resulting from abnormalities in left-right (LR) body patterning, has features suggesting that many cases fall into this category. In this setting, appropriate model systems may provide a means to support implication of specific genes. By high-resolution genotyping of 262 Htx subjects and 991 controls, we identify a twofold excess of subjects with rare genic copy number variations in Htx (14.5% vs. 7.4%, $P = 1.5 \times 10^{-4}$). Although 7 of 45 Htx copy number variations were large chromosomal abnormalities, 38 smaller copy number variations altered a total of 61 genes, 22 of which had *Xenopus* orthologs. In situ hybridization identified 7 of these 22 genes with expression in the ciliated LR organizer (gastrocoel roof plate), a marked enrichment compared with 40 of 845 previously studied genes (sevenfold enrichment, $P < 10^{-6}$). Morpholino knockdown in *Xenopus* of Htx candidates demonstrated that five (NEK2, ROCK2, TGFBR2, GALNT11, and NUP188) strongly disrupted both morphological LR development and expression of *pitx2*, a molecular marker of LR patterning. These effects were specific, because 0 of 13 control genes from rare Htx or control copy number variations produced significant LR abnormalities ($P = 0.001$). These findings identify genes not previously implicated in LR patterning.

cardiac development | *Xenopus tropicalis* | embryo

Congenital heart disease (CHD) is the most common major birth defect, affecting ~1% of live births, yet the cause of these lesions remains elusive. Although there is extensive evidence from epidemiologic, twin, and animal model studies supporting strong genetic contributions to CHD, only a small fraction of disease risk has been explained at the molecular level (1). Heterotaxy (Htx) is a severe form of CHD (2), in which normal left-right (LR) asymmetry is not properly established, leading to malformation of any organ that is asymmetric along the LR axis (Fig. 1). During embryonic development, cardiac precursor cells form a symmetric heart tube that undergoes rightward looping to form the geometric framework for the normal four-chambered heart. Defects in looping result in a spectrum of complex CHD in ~90% of Htx patients (3). CHD associated with Htx still has relatively poor survival, despite surgical management.

Studies in model systems have established a remarkably well-conserved genetic program governing patterning of the vertebrate LR axis (4–6) and cardiac development. LR asymmetry is established during gastrulation at the node (LR organizer) via dynein-driven, directional beating of cilia. Cilia beating results in leftward flow of extraembryonic fluid (nodal flow), which induces nodal signaling and Pitx2 expression in the left lateral-plate mesoderm (7, 8). Abnormal LR development leads to a striking and specific molecular and anatomic phenotype in all vertebrate embryos; a network of genes involved in the formation and function of the ciliated LR organizer that is conserved across all vertebrates has been described; however mutations in identified genes account for less than 10% of affected Htx subjects (9–18).

A major limitation in identifying causative genes in Htx is the paucity of families segregating highly penetrant alleles, and the high locus heterogeneity, which has limited the ability to map disease loci. Because of the marked impairment in reproductive fitness, some fraction of Htx could be caused by very rare, highly penetrant, dominant mutations.

Although such mutations have historically been difficult to identify, recent advances have improved the ability to detect these. For example, the use of quantitative interrogation of dense sets of SNPs has dramatically improved the ability to detect small copy number variants (CNVs) (19, 20). The significance of such rare mutations can be difficult to establish in the setting of high locus heterogeneity, as is the case for Htx, where discovering a second hit in the same gene in a small cohort is unlikely. Alternatively, their significance can potentially be assessed in high-throughput model systems. We have used *Xenopus tropicalis*, motivated by a conserved mechanism of LR development and prior use of this animal model system for robust cardiac and gut-looping assays. Moreover, *Xenopus* cardiac morphology is more similar to human than fish-human similarity (e.g., the presence of atrial septation), and its relatively compact diploid genome (1.5 Gb) retains substantial synteny to human, simplifying the identification of orthologous genes (21–23). Additionally, the ability to produce large numbers of embryos and the absence of recent genome duplications facilitates screening by morpholino (MO) knockdown technology (23, 24).

Results

Rare CNVs Are Overrepresented in Htx. We genotyped samples from 262 subjects with Htx, defined as any arrangement of organs across the LR axis differing from complete situs solitus or complete situs inversus (Fig.1 and Table S1). Because there is evidence that human mutations in known LR patterning genes can cause isolated transposition of the great arteries, we included patients with isolated transposition of the great arteries in our cohort (17, 25).

Author contributions: R.P.L., M.K.K., and M.B. designed research; K.A.F., M.C., M.K.K., and M.B. performed research; S.M.W., J.W.B., and J.A.T. contributed new reagents; K.A.F., M.C., R.P.L., M.K.K., and M.B. analyzed data; and K.A.F., R.P.L., M.K.K., and M.B. wrote the paper.

The authors declare no conflict of interest.

Freely available online through the PNAS open access option.

[1]To whom correspondence may be addressed. E-mail: martina.brueckner@yale.edu, mustafa.khoka@yale.edu, or richard.lifton@yale.edu.

This article contains supporting information online at www.pnas.org/lookup/suppl/doi:10.1073/pnas.1019645108/-/DCSupplemental.

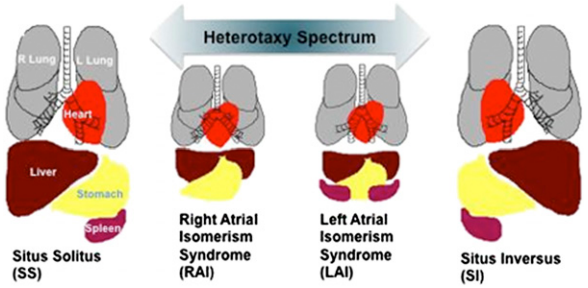

Fig. 1. Anatomy in human heterotaxy. Situs solitus (SS). The cardiac apex is oriented leftward, the right lung is trilobed, the left bilobed, the liver is on the right, and the stomach and spleen are on the left. Right atrial isomerism (RAI). Both lungs are trilobed, the liver is midline, and there is asplenia. Orientation of the cardiac apex is random, and complex CHD is found in >90% of affected patients. Left atrial isomerism (LAI). Both lungs are bilobed, the liver is midline, and there are multiple spleens. Orientation of the cardiac apex is random, and complex CHD is found in 80 to 90% of affected patients. Situs inversus (SI). Exact mirror-image of SS: the cardiac apex is rightward, there is a bilobed right lung and a trilobed left lung, the liver is on the left, and the stomach and spleen are on the right.

To identify CNVs from SNP genotype intensities, we used a likelihood-ratio based algorithm (26). In brief, quantitative intensity values of SNPs previously known to be present at 0, 1, 2, or 3 copies were used to determine the mean and SD of SNP intensities for each class. We then determined the likelihood ratio that a SNP with a given intensity has a copy number other than 2. The likelihood ratios for consecutive SNPs are strung together to assess the likelihood that segments of a given length represent a copy number other than 2. Applying this algorithm to independent test data sets showed that 0 copy variants (homozygous deletions) can be highly specifically called by characteristic intensity values with two or more consecutive SNPs, one copy variant (heterozygous deletions) by eight or more consecutive SNPs, and three copy variants (duplications) by 10 or more consecutive SNPs. Supporting data from B-allele frequencies were required to make CNV calls (i.e., loss of heterozygosity for heterozygous deletions or shift of the nonhomozygous SNP B-allele fractions from 0.5 to 0.33 and 0.66 for duplications) (Fig. 2 and Fig. S1).

To enrich for CNVs likely to have functional effect, we focused on genic CNVs, comprising deletions of at least one coding exon, and duplications that either encompassed an entire coding region or which produced an internal exon duplication. These genic CNVs were annotated for novelty and excluded from further consideration if they were found to have 5% or more overlap with any CNVs, either in the Database of Genomic Variants (http://projects.tcag.ca/variation/) (27) or in a set of 3,000 control subjects not known to have CHD. We assessed specificity by attempting to confirm the 17 smallest novel CNVs from this set (CNVs encompassing 19 or fewer SNPs) by quantitative PCR; this set included seven deletions and 10 duplications. All but a single 10-SNP duplication were confirmed (*Methods*).

We identified 45 previously unrecorded genic CNVs in 39 different subjects (Fig. 2 and Table S2). These CNVs included 16 heterozygous genic deletions, 25 complete duplications of at least one gene, and four internal genic duplications. These CNVs were in two size distributions: 38 were relatively small events, affecting one to five genes (27–1,488 kb, mean 2.1 genes per CNV), and seven were larger chromosomal abnormalities, each affecting > 90 genes (6–25 Mb, mean >250 genes per CNV). Many more Htx cases than controls had rare genic CNVs [38 of 262 Htx subjects (14.5%) versus 73 of 991 controls (7.4%), $P = 1.5 \times 10^{-4}$, ratio 2.0:1], consistent with CNVs playing a significant role in Htx development in some patients.

We focused further evaluation on the 38 CNVs of smaller size, anticipating that these may identify single genes with large effect on Htx risk. None of the 61 genes altered by these CNVs had been previously implicated in human Htx or any model of LR patterning. However, we did find genes in pathways previously linked to LR development, including 14 genes in either the ciliary proteome, zinc-finger transcription factor family, or TGF-β signaling pathway (28–30). Remarkably, despite the small cohort size, we found that TGF-β receptor 2 (TGFBR2) was affected twice by unique opposite-state CNVs in two unrelated patients (independent deletion and duplication of TGFBR2) (Fig. 2*A*).

Htx CNV Gene Expression Points to a Role in LR Development. To further analyze the 61 candidates, we undertook a screen in *X. tropicalis*, a robust model for studying LR patterning. We used expression analysis to prioritize genes for investigation, focusing on expression in the ciliated LR organizer [posterior notochordal plate or "node" in mouse, gastrocoel roof plate (GRP) in *Xenopus*], the kidney (which has prominent cilia), and the cardiovascular system. Of the 61 genes altered by novel CNVs, 22 had orthologs in *X. tropicalis*, with high sequence similarity and iden-

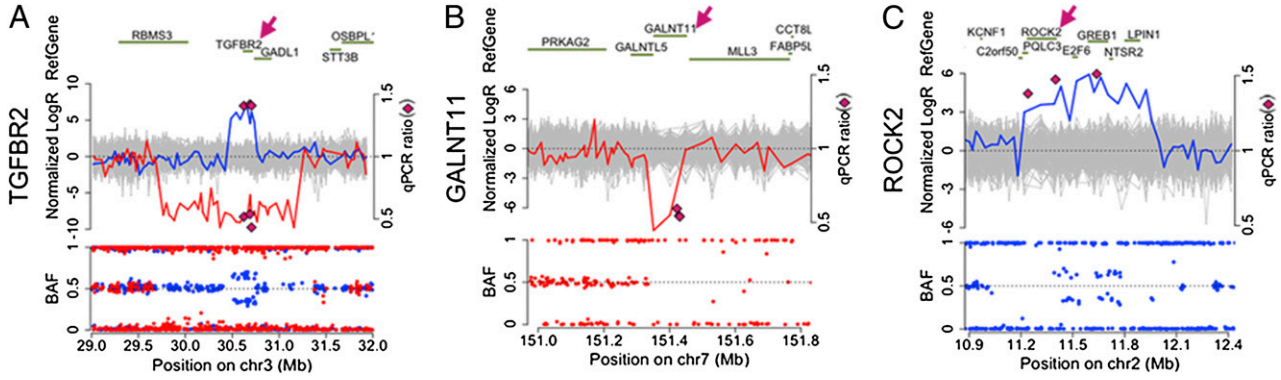

Fig. 2. Rare genic deletions and duplications in Htx patients. Results of Illumina genotyping and qPCR are shown for four CNVs at three loci that contain genes implicated in Htx. In all panels, genes in the indicated chromosome segment are shown and genes implicated in Htx are denoted by arrows. Data from subjects with deletion or duplications are shown in red or blue, respectively, and the remaining Htx subjects are depicted in gray. (*Upper*) Probe intensities in consecutive 10-SNP windows normalized to a mean of 0 and SD of 1 from values in the remaining Htx subjects. *P* values supporting CNVs are shown in Table S1. Ratios of results of qPCR in index cases compared with controls are shown as red diamonds. (*Lower*) B-allele fraction (BAF) of SNPs across the interval. Arrows indicate locations of implicated LR genes. (*A*) Independent deletion and duplication affecting TGFBR2 in subjects 28 and 139, respectively. (*B*) Deletion of first three exons of GALNT11 in subject 257. (*C*) Duplication of ROCK2 in subject 152.

tical neighboring genes. We examined their developmental expression patterns by whole-mount in situ hybridization (WMISH) at three developmental stages: neurula (stages 15–19, during which symmetry at the GRP is first broken) (Fig. 3*V*), tailbud (stages 26–29, during which cardiac tube fusion occurs) (Fig. 3*W*), and stages 33 to 36 (during which cardiac looping occurs) Fig. 3*X*). WMISH was successful for 20 of these genes. Seven genes exhibited nearly ubiquitous expression above that observed in sense controls (Fig. S2*A*), and the remaining 13 had more localized expression patterns (Fig. 3 and Fig. S2). Of these, seven genes (*tgfbr2*, *rock2*, *galnt11*, *lrrc8a*, *nek2*, *nup188*, and *greb1*) had expression patterns consistent with a potential role in LR and cardiovascular development, with expression in at least two relevant domains: five of these localized to the GRP (Fig. 3 *A*, *D*, *G*, *J*, and *M*), two were prominently expressed in the early heart (Fig. 3 *B*, *C*, *E*, and *F*), and five were expressed in the developing kidney (Fig. 3 *H*, *I*, *L*, *N*, *O*, *Q*, *R*, and *T*). GRP expression was highly enriched in the Htx gene set. In comparison, WMISH of 845 genes (http://*xenopus*.nibb.ac.jp) shows 40 with GRP expression; GRP-expressed genes are thus more than sevenfold enriched among rare Htx CNVs ($P = < 10^{-6}$). In addition, we identified 15 genes without *Xenopus* orthologs that had previous developmental expression studies in one or more vertebrate species, and none had noteworthy expression patterns. Inclusion of these 15 genes in the analysis of GRP/node enrichment in rare Htx CNVs continues to show significant enrichment (4.3-fold enrichment, $P = 2 \times 10^{-4}$).

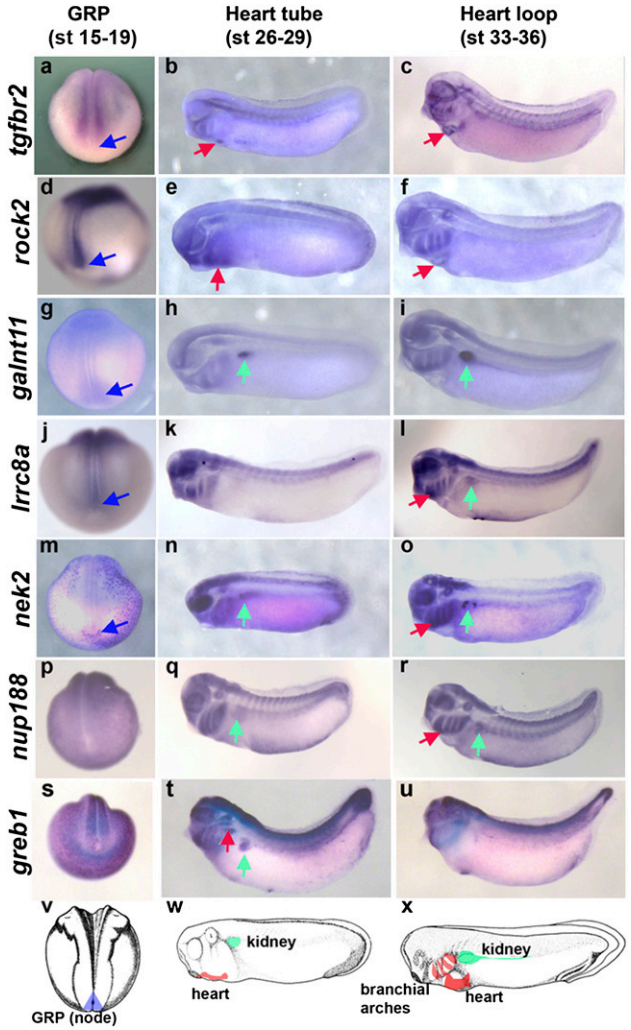

Fig. 3. WMISH analysis. (*A–U*) Results of in situ hybridization at three stages are shown for seven genes showing patterns of interest. These genes show expression in one or more of the following: GRP (blue arrows); heart or branchial arches (red arrows); kidney (green arrows). Stage 15 to 19 embryos are viewed dorso-posteriorly with anterior to the top to examine GRP expression (shown schematically in *V*). Stage 26 to 29 and stage 33 to 36 embryos are viewed laterally with anterior to the left (shown schematically in *W* and *X*, respectively).

Knockdown in *X. tropicalis* Validates Htx Genes. Based on the suggestive expression data of these seven genes, we examined the effect of MO knockdown of these candidates on LR patterning. This strategy was motivated by previous studies demonstrating dosage sensitivity for many chromosomal regions containing CHD genes, including: 22q11 (conotruncal defects) (31), 8p23 [AV septal defects, Tetralogy of Fallot TOF)] (32), 7q11 (supravalvar aortic stenosis-del and PDA-dup) (33), 16p13 encompassing the *CRBBP* gene (Rubinstein-Taybi syndrome-del and septal defects-dup) (34), and 1q21.1 (TOF) (35). Similarly, we identify independent patients with deletion and duplication affecting the region on chromosome 3 encompassing TGFBR2. Taken together, these data suggest that for many critical genes, either too much or too little gene activity results in CHD (36, 37).

As positive controls for the MO experiments, we tested *dnah9* and *ift88*, both previously reported to give robust LR phenotypes in *Xenopus* (38). As negative controls, we injected the standard negative control MO along with evaluation of dye-injected and uninjected controls. To address specificity of MO effects on LR phenotypes, we also examined 13 additional control genes: five genes from rare CNVs in Htx patients who did not have suggestive expression patterns (*igfbp5*, *laptm5*, *runx2*, *smarcal1*, *tpk1*, expression control) (Fig. S3), and eight genes from rare CNVs in controls (*aldh1a1*, *cryzl1*, *gdf7*, *grik1*, *ccbl1*, *myh6*, *pdgfc*, *trat1*, non-Htx control) (Fig. S3).

All MOs were injected at the one-cell stage, and embryos were raised to stage 45/46, at which point heart- and gut-looping morphology were assessed. Because complete loss of function of some of these genes causes early embryonic lethality, we titrated doses of each MO from 0.5 to 20 ng per embryo and selected doses that minimally affected antero-posterior and dorso-ventral development for each. Final experimental doses for these stages ranged from 0.5 ng (60 fmol) to 4 ng (480 fmol) per embryo; standard control MO was injected at 8 ng per embryo. Heart looping was scored by established methods (21) as D-looped (normal) (Fig. 4*A*), L-looped (reversed) (Fig. 4*C*), or A-looped (midline/anterior-loop) (Fig. 4*B*). Gut looping was scored as either normal or abnormal (Fig. 4 *D* and *E*). At least 54 (mean n = 78) embryos were scored for each MO. Morphant embryos were scored by two independent readers blinded to group status, with 95% concordance of scoring for heart and gut phenotypes.

Five of the seven Htx candidate MOs had striking effects on LR patterning, with abnormally looped hearts in 24 to 36% of embryos. The values in these five test morphants were equal to or greater than the effects of positive control MOs, and significantly greater than the standard negative control (all $P \leq 0.0001$, for difference in heart looping) (Fig. 4*G*). Similarly, abnormal gut looping was seen with these same five MOs, with abnormal looping in 39 to 91% of embryos, again similar to positive controls and significantly greater than standard negative control (all $P \leq 0.0001$) (Fig. 4*H*). Morphants of the two remaining test genes, *greb1* and *lrrc8a*, gave no significant LR looping phenotype (Figs. S3 and S4). Notably, both *greb1* and *lrrc8a* were in CNVs that include another gene that gave a strong LR phenotype by MO knockdown (*nup188* and *rock2,* respectively) (Fig. S4, red arrows). The absence of a strong LR phenotype in the *greb1* and *lrrc8a* morphants is consistent with a model in which a single gene in these multiple gene CNVs contributes to Htx. These striking effects on LR morphology showed specificity, because

none of the 13 additional control MOs had a significant effect on LR patterning (all $P > 0.4$ vs. standard negative control) (Fig. S3). The difference in the frequency of LR defects between the test and control groups was highly significant (5/7 vs. 0/13, $P = 0.001$ by Fisher's exact test).

Htx can result from either a global effect on LR patterning or a heart-field–specific effect on cardiac looping. Because the five genes that showed abnormal LR patterning with MO knockdown affected both heart and gut patterning, we expected that they should act upstream in the pathway. We tested this by examining expression of an early marker of global LR patterning, the transcription factor *pitx2*, which is normally induced by *nodal* signaling on the left side of the embryo, but inhibited on the right side (39). We assayed *pitx2* expression in morphants by WMISH at stages 28 to 30 (before heart-tube looping) using MO doses that minimally disrupted antero-posterior and dorso-ventral development at this stage (0.5–8 ng per embryo). Embryos were scored as showing left-sided, right-sided, bilateral, or absent *pitx2* expression (Fig. 5). At least 45 (mean $n = 74$) embryos were scored in each group. Negative control morphants showed 88% strong left-sided *pitx2* expression, and 12% abnormal patterns. In contrast, consistent with prior reports (40), the positive control *dnah9* morphants showed 35% abnormal *pitx2* expression ($P < 2 \times 10^{-4}$). All five test morphants that produced abnormal heart and gut patterning also produced abnormalities in *pitx2* expression (30–52% abnormality; all $P < 0.002$) (Fig. 5).

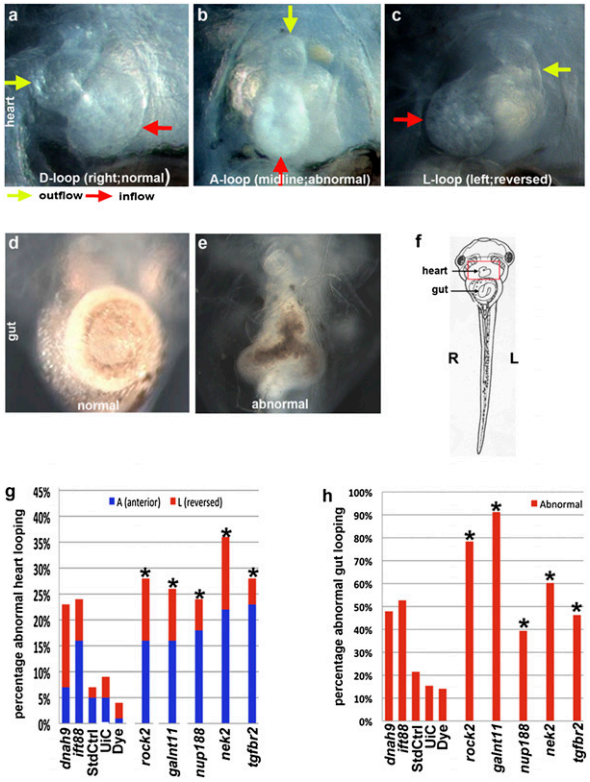

Fig. 4. LR abnormalities from MO knockdown in *X. tropicalis*. MOs were injected at the one-cell stage and heart and gut looping were assayed in tadpoles at stage 45/46. Views are from the ventral aspect, shown in schematic form in *F*. (*A*) Heart (area outlined in red box as in schematic in *F*) showing normal D-looping. The inflow (red arrow) is on the tadpole's left, the outflow tract (yellow arrow) is on the tadpole's right. (*B*) Heart showing abnormal, anterior, A-looping. The inflow (red) and outflow (yellow) are both at the midline, with no discernible LR orientation. (*C*) Heart showing abnormal, reversed, L-looping. The inflow (red) is on the tadpole's right, the outflow (yellow) is on the tadpole's left. (*D*) Normal clockwise rotation of the gut. (*E*) Abnormal gut rotation. (*F*) Schematic of *Xenopus* tadpole at stage 45/46; ventral view with anterior to the top; arrows indicate heart and gut. (*G*) Heart looping in MO knockdown tadpoles. Both *dnah9* and *ift88* are positive controls; standard control MO (StdCtrl), uninjected control (UiC), and dye-injected (Dye) are negative controls. Bars show the total percentage of abnormally looped hearts: divided into A-loop (blue) and L-loop (red). (*H*) Gut looping in MO knockdown tadpoles. Both *dnah9* and *ift88* MOs are used as positive controls; StdCtrl, UiC, and Dye are used as negative controls. Red bars show the the percent of abnormal gut loops. Heart and gut looping were analyzed by two independent readers blinded to group status with 95% concordance. $*P < 10^{-4}$ vs. StdCtrl.

Discussion

We have identified rare genic CNVs in Htx patients and demonstrated the effect of specific genes in these CNVs on LR development using MO knockdown in *X. tropicalis*, implicating mutations in five genes. The evidence supporting phenotypic effect of these mutations includes highly significant enrichment of rare genic CNVs in Htx patients; highly significant enrichment in these CNVs of genes with expression in the GRP; and specific production of morphologic and molecular LR abnormalities by MO knockdown of these genes. Although the latter evidence indicates that modulation of these single genes is sufficient to produce LR phenotypes in *Xenopus*, we presume but cannot be certain that the same is true in humans. In addition, we found seven relatively large chromosomal abnormalities in these Htx patients, suggesting one or more genes in these CNVs also contribute to Htx. Included in this group was one 8p deletion

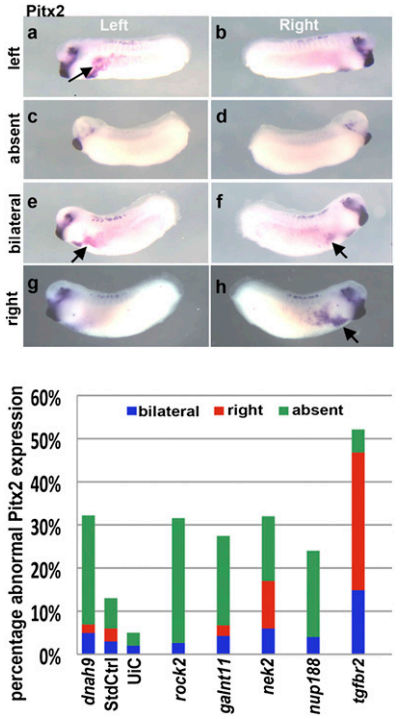

Fig. 5. Analysis of *pitx2* expression in stage 28 to 30 *Xenopus* embryos. Embryos are viewed laterally from the left (first column) and the right (second column). Note normal, bilateral *pitx2* expression in the head region in all embryos. (*A*) Expression of *pitx2* is normally in the left lateral plate mesoderm (LPM, arrow). (*B*) Same normal embryo showing absent *pitx2* expression in the right LPM. (*C* and *D*) Absent *pitx2* expression. No *pitx2* mRNA is found in the left or right LPM. (*E* and *F*) Bilateral *pitx2* expression. The *pitx2* mRNA is found in both left and right LPM (arrows). (*G* and *H*) Right *pitx2* expression: *pitx2* mRNA is absent from the left LPM, present in the right LPM. (*Graph*) Summary of *pitx2* mRNA expression in MO knockdown embryos: *dnah9* is a positive control; StdCtrl, and UiC are negative controls. Bars show the percent of abnormal *pitx2* expression and are divided into blue (bilateral), red (right), and green (absent) LPM *pitx2* expression.

that included GATA4, which is known to result in diverse CHD phenotypes (41). These findings collectively demonstrate that independent rare CNVs are likely related to pathogenesis in at least 3.8% of Htx patients; because there is no expression data for 26 of the genes in rare genic Htx CNVs, this number is likely underestimated. Although parental samples were not available in this study, the demonstration that a high proportion of the CNVs containing implicated genes were de novo events would strengthen the evidence for genetic causation and should be an element of future studies. Rare CNVs have also been suggested to play a role in diverse outflow tract lesions, including TOF (35). Because CNVs comprise a small fraction of mutation burden in most genes, additional mutations with large effect will likely contribute to Htx, motivating efforts to identify them with technologies such as whole-exome sequencing (26).

It is noteworthy that all five genes identified in this study are previously unrelated to LR patterning. This finding suggests that prior studies of LR development have only uncovered a small fraction of the genes required for LR patterning and may explain why candidate gene resequencing has identified mutations in only 8 to 10% of Htx patients. In addition, diverse clinical phenotypes within the Htx spectrum are seen among patients with these CNVs (Table S1). These phenotypes include transposition of the great arteries, abdominal situs inversus, asplenia/polysplenia, partial anomalous pulmonary venous return, and aortic coarctation.

Among the five genes, *NEK2* (never in mitosis kinase 2) (42) and *ROCK2* (Rho-associated kinase 2) (43) are found in the ciliary proteome. Cilia play a pivotal role in the earliest events in LR development, and ciliary defects underlie a disproportionate number of laterality defects in mice, frogs, zebrafish, and humans (44). Mutations producing ciliary immotility cause primary ciliary dyskinesia, often featuring Htx (12). Mutations expected to disrupt centrosome function, ciliary biogenesis, or ciliary signaling, cause syndromes such as Bardet-Biedl syndrome (45) and Meckel-Gruber syndrome (46), featuring developmental defects including CHD. Nek2 is a member of a family of NIMA-related kinases implicated in cell cycle control and are defective in mouse cystic kidney disease, a known ciliary disorder (47). Knockdown of Nek2 in mice results in failure to develop beyond the eight-cell stage (48).

We also identified mutations in genes of the TGF-β signaling pathway. Most notably, we found two subjects with mutations in TGFBR2: one duplication and one deletion. The TGF-β ligand nodal is critical in LR patterning (5); studies have largely focused on the nodal/activin branch of TGF-β signaling. Our findings implicate the TGF-β/TGFBR branch of this signaling network in LR development, consistent with prior evidence that TGF-β1 overexpression in *X. laevis* resulted in LR defects (49). The finding of both a rare duplication and deletion of TGFBR2 suggests that either increased or decreased signaling results in Htx, similar to other CHD genes (50). Point mutations in TGFBR2 cause Loeys-Dietz syndrome, which leads to aortopathy and a spectrum of CHD (51). Additionally, cardiac-specific deletion of TGFBR2 in mice results in abnormal heart looping (52). Together with our data showing abnormal *pitx2* expression in *tgfbr2* morphants, this finding suggests that TGF-β signaling functions both in global LR axis formation and at later stages in looping morphogenesis. It is noteworthy that ROCK2 may provide a link between cilia and TGF-β signaling: in addition to being part of the ciliary proteome, ROCK2 inhibits mesoderm induction in zebrafish embryos by binding to and accelerating the lysosomal degradation of TGFBR1 (43). A general inhibitor of Rho kinases was shown to affect LR development in chick (53), and after submission of this article, rock2b was implicated in LR patterning in zebrafish by MO knockdown, supporting the evolutionary conservation of this gene's role in LR patterning (54).

GALNT11, which encodes a glycosyl transferase, was also identified in this screen. This finding is noteworthy in that *GALNT11* has highly conserved domains similar to another family member, GALNT-like1, which has recently been shown to inhibit nodal signaling by glycosylating activin receptor 1B, preventing it from associating with activin receptor (55). This observation suggests *GALNT11* may play a related role in modulating TGF-β signaling.

The final gene implicated in our screen is *NUP188*, a component of the nuclear pore complex. Nucleoporins function in transport of macromolecules between the nucleus and cytoplasm and in transcriptional regulation (56, 57). *NUP188* is thought to play a role in preventing the passage of integral membrane proteins into the nucleus (58). How *NUP188* functions in LR development remains to be elucidated.

In summary, these findings support the notion that many apparently sporadic cases of Htx have substantial contribution from rare genetic variation. They motivate further efforts to identify rare mutations in such patients. We believe the approach we have taken can be extended to other human developmental disorders, especially those for which morphology is conserved in a high-throughput system. We anticipate such studies will advance the understanding and treatment of Htx and other human birth defects in the coming years.

Methods

Study Populations. We analyzed 262 heterotaxy patients (by genotype, 120 cluster with subjects of European ancestry, 104 Hispanic, 19 African Americans, 19 all others). Patients with isolated D- and L-transposition of the great arteries were included. Coded DNA samples were obtained from two participating centers, Baylor College of Medicine (Houston, TX) and Yale University School of Medicine (New Haven CT). The study was approved by the Yale and Baylor Institutional Review Boards. Patients were previously evaluated for mutation in NODAL, ZIC3, CFC1, LEFTYA, LEFTYB, and ACVR2B. Patients identified to have novel genic CNVs in our study did not have mutations in these genes.

We also analyzed a control cohort comprising 999 subjects of European ancestry. We genotyped the controls on the same platform and subjected them to the same QC steps and CNV analysis algorithms and parameters used for CNV discovery in the patient cohort. None of the controls had congenital heart disease.

CNV Discovery and Novelty Assessment. Two-hundred eighty-eight Htx samples were genotyped on the Illumina 610Quad Beadchip platform (~620,000 SNP markers plus ~60,000 CNP markers; average call rate: 99.77%, SD: 0.1%). Of 288 Htx samples, 262 passed initial QC and were submitted for CNV discovery. In the control cohort, 991 of 999 passed initial QC. CNVs were discovered using a likelihood ratio-based algorithm, as previously described (26), using thresholds of 8 and 10 consecutive probes for heterozygous deletions and duplications, respectively. In these high-confidence CNVs, we assessed novelty by comparing their coordinates to known CNVs in the Database of Genomic Variants and CNVs called in 3,000 internal controls. CNVs were discarded if at least 5% of their length overlapped any CNV in these two databases. Ninety-six CNVs passed this test and were considered high-confidence unique variants.

Quantitative PCR Validation. For each tested CNV, at least two primer pairs were designed within the boundaries of the CNV region. Additionally, a primer set was designed to amplify a known copy-neutral segment of the *ZNF423* gene. The ratio of amplification of the test locus to amplification of the *ZNF423* diploid locus in patients and two sets of pooled controls were compared in triplicate amplifications performed in parallel. In the absence of deletion/duplication, the ratio of test locus:control locus in cases are expected to be no different from the ratio in pooled controls (mean value 1.0). In contrast, these ratios should approximate 0.5 for heterozygous deletions and 1.5 for heterozygous duplications. Consistent results in triplicate samples with at least two primer pairs were required to declare a conclusive result. Quantitative PCR was performed on 23 loci (14 duplications, 9 deletions), 17 of which were the smallest (<19 probes) rare genic CNVs. All but one 10-probe duplication produced qPCR results concordant with the copy-number state predicted by our CNV detection algorithm (>95% specificity).

***Xenopus* Analysis.** *X. tropicalis* orthologs of human genes were identified using Metazome (www.metazome.com) or Xenbase (www.xenbase.org)

Web sites. In each case, evidence of synteny to the human genome was required to confirm orthology. One gene, *CETN1*, is a member of a highly homologous multigene family and was not investigated further. WMISH was performed as previously described (24). We identified GRP expression in control genes from a public database (http://xenopus.nibb.ac.jp/). MOs were injected at the one-cell stage and embryos scored at stage 45/46 for LR phenotypes and stages 26 to 29 for *pitx2*. Clones used for generating antisense probes are available upon request. *Xenopus* procedures were reviewed and approved by Yale's Institutional Animal Care and Use Committee, which is Association for Assessment and Accreditation of Laboratory Animal Care-accredited. Additional detailed methods and a summary of MO sequences and doses are available in *SI Methods* and Table S3.

Statistical Analysis. Statistical comparisons between groups were by χ^2 statistics unless expected cell frequencies were less than 5, in which case Fisher's exact test was used.

ACKNOWLEDGMENTS. We thank the patients and families who participated in this study and the staff of the Yale West Campus Center for Genomic Analysis for their contributions to this project, Carol Nelson-Williams for helpful discussions and advice, and Michael Slocum and Sarah Kirschner for animal husbandry. This study was supported by National Institutes of Health Grants R01HD045789 and R01HL093280 (to M.B.) and R01DE018824 and R01DE018825 (to M.K.K.). R.P.L. is an Investigator of The Howard Hughes Medical Institute.

1. Pierpont ME, et al.; American Heart Association Congenital Cardiac Defects Committee, Council on Cardiovascular Disease in the Young (2007) Genetic basis for congenital heart defects: Current knowledge: A scientific statement from the American Heart Association Congenital Cardiac Defects Committee, Council on Cardiovascular Disease in the Young: Endorsed by the American Academy of Pediatrics. *Circulation* 115:3015–3038.
2. Cohen MS, et al. (2007) Controversies, genetics, diagnostic assessment, and outcomes relating to the heterotaxy syndrome. *Cardiol Young* 17(Suppl 2):29–43.
3. Taketazu M, Lougheed J, Yoo SJ, Lim JS, Hornberger LK (2006) Spectrum of cardiovascular disease, accuracy of diagnosis, and outcome in fetal heterotaxy syndrome. *Am J Cardiol* 97:720–724.
4. Levin M, Johnson RL, Stern CD, Kuehn M, Tabin C (1995) A molecular pathway determining left-right asymmetry in chick embryogenesis. *Cell* 82:803–814.
5. Shiratori H, Hamada H (2006) The left-right axis in the mouse: From origin to morphology. *Development* 133:2095–2104.
6. Bisgrove BW, Morelli SH, Yost HJ (2003) Genetics of human laterality disorders: Insights from vertebrate model systems. *Annu Rev Genomics Hum Genet* 4:1–32.
7. Nonaka S, et al. (1998) Randomization of left-right asymmetry due to loss of nodal cilia generating leftward flow of extraembryonic fluid in mice lacking KIF3B motor protein. *Cell* 95:829–837.
8. McGrath J, Somlo S, Makova S, Tian X, Brueckner M (2003) Two populations of node monocilia initiate left-right asymmetry in the mouse. *Cell* 114:61–73.
9. Bartoloni L, et al. (2002) Mutations in the *DNAH11* (axonemal heavy chain dynein type 11) gene cause one form of situs inversus totalis and most likely primary ciliary dyskinesia. *Proc Natl Acad Sci USA* 99:10282–10286.
10. Gebbia M, et al. (1997) X-linked situs abnormalities result from mutations in ZIC3. *Nat Genet* 17:305–308.
11. Karkera JD, et al. (2007) Loss-of-function mutations in growth differentiation factor-1 (GDF1) are associated with congenital heart defects in humans. *Am J Hum Genet* 81: 987–994.
12. Kennedy MP, et al. (2007) Congenital heart disease and other heterotaxic defects in a large cohort of patients with primary ciliary dyskinesia. *Circulation* 115:2814–2821.
13. Kosaki K, et al. (1999) Characterization and mutation analysis of human LEFTY A and LEFTY B, homologues of murine genes implicated in left-right axis development. *Am J Hum Genet* 64:712–721.
14. Kosaki R, et al. (1999) Left-right axis malformations associated with mutations in ACVR2B, the gene for human activin receptor type IIB. *Am J Med Genet* 82:70–76.
15. Roessler E, et al. (2009) Cumulative ligand activity of NODAL mutations and modifiers are linked to human heart defects and holoprosencephaly. *Mol Genet Metab* 98: 225–234.
16. Schwabe GC, et al. (2008) Primary ciliary dyskinesia associated with normal axoneme ultrastructure is caused by DNAH11 mutations. *Hum Mutat* 29:289–298.
17. van Bon BW, et al. (2008) Transposition of the great vessels in a patient with a 2.9 Mb interstitial deletion of 9q31.1 encompassing the inversin gene: clinical report and review. *Am J Med Genet A* 146A:1225–1229.
18. Sutherland MJ, Ware SM (2009) Disorders of left-right asymmetry: Heterotaxy and situs inversus. *Am J Med Genet C Semin Med Genet* 151C:307–317.
19. Conrad DF, et al.; Wellcome Trust Case Control Consortium (2010) Origins and functional impact of copy number variation in the human genome. *Nature* 464: 704–712.
20. Craddock N, et al.; Wellcome Trust Case Control Consortium (2010) Genome-wide association study of CNVs in 16,000 cases of eight common diseases and 3,000 shared controls. *Nature* 464:713–720.
21. Blum M, et al. (2009) *Xenopus*, an ideal model system to study vertebrate left-right asymmetry. *Dev Dyn* 238:1215–1225.
22. Schweickert A, et al. (2007) Cilia-driven leftward flow determines laterality in *Xenopus*. *Curr Biol* 17:60–66.
23. Hellsten U, et al. (2010) The genome of the Western clawed frog *Xenopus tropicalis*. *Science* 328:633–636.
24. Khokha MK, et al. (2002) Techniques and probes for the study of *Xenopus tropicalis* development. *Dev Dyn* 225:499–510.
25. De Luca A, et al. (2010) Familial transposition of the great arteries caused by multiple mutations in laterality genes. *Heart* 96:673–677.
26. Choi M, et al. (2009) Genetic diagnosis by whole exome capture and massively parallel DNA sequencing. *Proc Natl Acad Sci USA* 106:19096–19101.
27. Iafrate AJ, et al. (2004) Detection of large-scale variation in the human genome. *Nat Genet* 36:949–951.
28. Avidor-Reiss T, et al. (2004) Decoding cilia function: Defining specialized genes required for compartmentalized cilia biogenesis. *Cell* 117:527–539.
29. Ostrowski LE, et al. (2002) A proteomic analysis of human cilia: Identification of novel components. *Mol Cell Proteomics* 1:451–465.
30. Pazour GJ, Agrin N, Leszyk J, Witman GB (2005) Proteomic analysis of a eukaryotic cilium. *J Cell Biol* 170:103–113.
31. Portnoï MF (2009) Microduplication 22q11.2: A new chromosomal syndrome. *Eur J Med Genet* 52:88–93.
32. Barber JC, et al. (2008) 8p23.1 duplication syndrome; a novel genomic condition with unexpected complexity revealed by array CGH. *Eur J Hum Genet* 16:18–27.
33. Van der Aa N, et al. (2009) Fourteen new cases contribute to the characterization of the 7q11.23 microduplication syndrome. *Eur J Med Genet* 52:94–100.
34. Thienpont B, et al. (2010) Duplications of the critical Rubinstein-Taybi deletion region on chromosome 16p13.3 cause a novel recognisable syndrome. *J Med Genet* 47: 155–161.
35. Greenway SC, et al. (2009) De novo copy number variants identify new genes and loci in isolated sporadic tetralogy of Fallot. *Nat Genet* 41:931–935.
36. Mefford HC, et al. (2008) Recurrent rearrangements of chromosome 1q21.1 and variable pediatric phenotypes. *N Engl J Med* 359:1685–1699.
37. Kontaridis MI, Swanson KD, David FS, Barford D, Neel BG (2006) PTPN11 (Shp2) mutations in LEOPARD syndrome have dominant negative, not activating, effects. *J Biol Chem* 281:6785–6792.
38. Schweickert A, et al. (2010) The nodal inhibitor coco is a critical target of leftward flow in *Xenopus*. *Curr Biol* 20:738–743.
39. Piedra ME, Icardo JM, Albajar M, Rodriguez-Rey JC, Ros MA (1998) Pitx2 participates in the late phase of the pathway controlling left-right asymmetry. *Cell* 94:319–324.
40. Vick P, et al. (2009) Flow on the right side of the gastrocoel roof plate is dispensable for symmetry breakage in the frog *Xenopus laevis*. *Dev Biol* 331:281–291.
41. Tomita-Mitchell A, Maslen CL, Morris CD, Garg V, Goldmuntz E (2007) GATA4 sequence variants in patients with congenital heart disease. *J Med Genet* 44:779–783.
42. Fry AM (2002) The Nek2 protein kinase: A novel regulator of centrosome structure. *Oncogene* 21:6184–6194.
43. Zhang Y, et al. (2009) Rock2 controls TGFbeta signaling and inhibits mesoderm induction in zebrafish embryos. *J Cell Sci* 122:2197–2207.
44. Eggenschwiler JT, Anderson KV (2007) Cilia and developmental signaling. *Annu Rev Cell Dev Biol* 23:345–373.
45. Nachury MV, et al. (2007) A core complex of BBS proteins cooperates with the GTPase Rab8 to promote ciliary membrane biogenesis. *Cell* 129:1201–1213.
46. Dawe HR, et al. (2007) The Meckel-Gruber Syndrome proteins MKS1 and meckelin interact and are required for primary cilium formation. *Hum Mol Genet* 16:173–186.
47. Mahjoub MR, Trapp ML, Quarmby LM (2005) NIMA-related kinases defective in murine models of polycystic kidney diseases localize to primary cilia and centrosomes. *J Am Soc Nephrol* 16:3485–3489.
48. Sonn S, Khang I, Kim K, Rhee K (2004) Suppression of Nek2A in mouse early embryos confirms its requirement for chromosome segregation. *J Cell Sci* 117:5557–5566.
49. Mogi K, et al. (2003) *Xenopus* neurula left-right asymmetry is respeficied by microinjecting TGF-beta5 protein. *Int J Dev Biol* 47:15–29.
50. Laitenberger G, Donner B, Gebauer J, Hoehn T (2008) D-transposition of the great arteries in a case of microduplication 22q11.2. *Pediatr Cardiol* 29:1104–1106.
51. Loeys BL, et al. (2005) A syndrome of altered cardiovascular, craniofacial, neurocognitive and skeletal development caused by mutations in TGFBR1 or TGFBR2. *Nat Genet* 37:275–281.
52. Jiao K, et al. (2006) Tgfbeta signaling is required for atrioventricular cushion mesenchyme remodeling during in vivo cardiac development. *Development* 133: 4585–4593.
53. Wei L, et al. (2001) Rho kinases play an obligatory role in vertebrate embryonic organogenesis. *Development* 128:2953–2962.
54. Wang G, et al. (2011) The Rho kinase Rock2b establishes anteroposterior asymmetry of the ciliated Kupffer's vesicle in zebrafish. *Development* 138:45–54.
55. Herr P, Korniychuk G, Yamamoto Y, Grubisic K, Oelgeschläger M (2008) Regulation of TGF-(beta) signalling by N-acetylgalactosaminyltransferase-like 1. *Development* 135: 1813–1822.
56. Kalverda B, Pickersgill H, Shloma VV, Fornerod M (2010) Nucleoporins directly stimulate expression of developmental and cell-cycle genes inside the nucleoplasm. *Cell* 140:360–371.
57. Capelson M, et al. (2010) Chromatin-bound nuclear pore components regulate gene expression in higher eukaryotes. *Cell* 140:372–383.
58. Theerthagiri G, Eisenhardt N, Schwarz H, Antonin W (2010) The nucleoporin Nup188 controls passage of membrane proteins across the nuclear pore complex. *J Cell Biol* 189:1129–1142.